JOURNAL OF GEOPHYSICAL RESEARCH, VOL. 88, NO. C4, PAGES 2662–2666, MARCH 20, 1983

On the Stratification of Turbulent Mixed Layers

L. MAHRT AND JEAN-CLAUDE ANDRÉ[1]

Atmospheric Sciences Department, Oregon State University, Corvallis, Oregon 97331

The vertical distribution of density or temperature is studied in turbulent boundary layers stratified by either salt or temperature and driven in an annulus by a rotating screen. With rapidly growing boundary layers the buoyancy flux due to entrainment becomes sufficiently large that the boundary layer is no longer well mixed. Stratification in the boundary layer is largest near the entrainment interface, corresponding to extension of the density transition into the turbulent boundary layer. The stratification in the rest of the boundary layer is smaller and nearly independent of height. The mean boundary layer stratification and structure and integral properties of the density distribution are found to be strongly dependent on the ratio of the entrainment rate to the turbulent velocity scale.

1. INTRODUCTION

Most analyses of laboratory mixing layers and associated modeling efforts have assumed that density or temperature stratification vanishes uniformly throughout the layer. Little effort has addressed how boundary layers, which are not completely well mixed, asymptotically approach a well-mixed state as turbulent activity becomes more effective. *André et al.* [1979] developed a similarity theory to describe the gradient of moisture in heated atmospheric boundary layers which are essentially well mixed in potential temperature. The recent similarity analysis of mixing layers by *Kundu* [1981] contains temperature stratification extending from the entrainment region into the boundary layer.

Deardorff and Willis [1982] suggest that the stratification of density or temperature in entraining laboratory boundary layers appears to increase with increasing values of the entrainment rate relative to the turbulent velocity scale. With sufficiently rapid entrainment relative to the turbulent intensity, the buoyancy flux due to entrainment creates density stratification in the boundary layer which cannot be eliminated by turbulent mixing. In fact, in the experiments of Deardorff and Willis, significant density gradients occurred if the entrainment rate exceeded about three percent of the surface friction velocity. Qualitatively similar phenomena are also observed in the tank experiments conducted by *Hopfinger and Linden* [1981] where significant density gradients appear when an imposed buoyancy flux exceeds a critical value relative to the turbulence generated by an oscillating grid. Failure to completely mix density and resulting stable stratification require reconsideration of the turbulence energy equation and resulting usual approach to modeling mixing layer growth (see *Stull* [1976], *Niiler and Kraus* [1977], *Artaz and André* [1980], and *Tennekes and Driedonks* [1981] for surveys of such approaches).

To study the existence and vertical structure of entrainment-induced stratification in the boundary layer and dependence on external parameters, we will analyze temperature and density data from the laboratory experiments of *Deardorff and Willis* [1982] and *Kantha* [1978]. In section 2 we define such unmixedness by taking advantage of the fact that in the data examined here, stratification approaches a constant value in at least half of the boundary layer adjacent to the solid surface. In the rest of the boundary layer the stratification increases toward the entrainment interface. In section 3 this variable stratification is included by evaluating integral properties, which avoids the problem of partitioning the boundary layer into specific zones.

2. OBSERVATIONAL EVIDENCE

Examples of typical smoothed density gradients in laboratory boundary layers are shown in Figures 1 and 2 for one of the two-layer salt-stratified experiments reported by *Kantha* [1978] and for one of the experiments conducted by *Deardorff and Willis* [1982] where density stratification is initially created by a linear temperature profile. In the former case the turbulent boundary layer remains stably stratified, as heavier fluid is entrained from the underlying salty quiescent layer into the upper freshwater mixing layer. In the latter case the relatively colder, turbulent layer is stably stratified by downward entrainment of warmer fluid, and there is an almost continuous temperature transition between the growing turbulent layer and the overlying laminar flow. In both cases the stratification in the boundary layer increases toward the interface, as modeled by *Kundu* [1981].

We shall analyze data collected by Deardorff and Willis, part of which appears in the work by *Deardorff and Willis* [1982] and part of which were kindly made available to us from their original listings and graphs. In their experiments the turbulent boundary layer is created by a rotating screen located at the bottom of the annulus and the density stratification is created by using either a linear temperature gradient of 1 K cm^{-1} or a two-layer system with salty water at the bottom and fresh water at the top. The data by *Kantha* [1978] were taken directly from his Figures 30–32 and 35–40 and Table 3. In his experiments the turbulent boundary layer is created by a rotating screen located at the top of the apparatus and the density stratification is created by a two-layer system.

To compare salt-stratified and temperature-stratified experiments, temperature T has been converted into density ρ by using a coefficient of thermal expansion

$$\alpha = -\frac{1}{\rho}\frac{\partial \rho}{\partial T}$$

[1]Now at the Centre National de la Recherche Météorologique, Toulouse, France.

Paper number 2C1768.
0148-0227/83/002C-1768$05.00

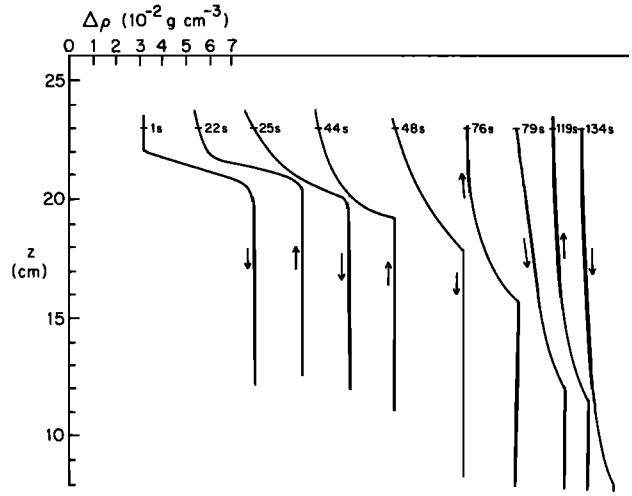

Fig. 1. Mean smoothed density profiles in the experiments of *Kantha* [1978]. Arrows indicate measurements taken during either upward or downward traverses.

which varies with temperature (Table 1). The profiles of density and temperature measured by Deardorff and Willis are essentially Eulerian, although the salt probe leads to horizontal averaging on a scale thought to be about 2 mm, while the response lag of thermistor leads to vertical averaging also on a scale of about 2 mm.

3. Similarity Analysis and Results

In the similarity analysis of *Kundu* [1981], temperature within the mixing layer is assumed to be of the form

$$T(\eta) = T_h + \Delta T\, G(\eta)$$

where T_h is the temperature on the quiescent edge of the interface, ΔT is the temperature change across the turbulent boundary layer, G is a similarity function of $\eta = z/h$ and independent of time, and h is the depth of the turbulent layer. With this similarity condition the scaled temperature gradient

$$\frac{\partial T}{\partial z}\frac{h}{\Delta T} = \frac{\partial G}{\partial \eta}$$

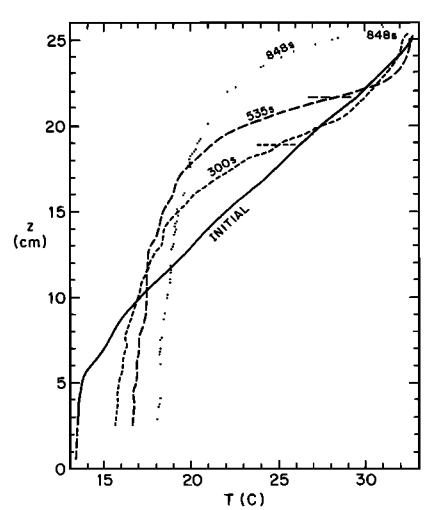

Fig. 2. Temperature profiles in the experiments of *Deardorff and Willis* [1982].

is independent of time, either when considered at a fixed nondimensional height z/h or when averaged over a fixed portion of the boundary layer between two levels of constant η. This restriction does not prohibit changes in the dimensional temperature gradient. For example, in the case of a two-layer fluid stratified by a temperature jump, the dimensional temperature gradient and $\Delta T/h$ decrease with time. In the work of *Kundu* [1981] the scaled temperature gradient $\partial G/\partial \eta$, although independent of time, could vary from case to case according to variations in different parameters such as the overall Richardson number. The similarity solutions presented by Kundu were in approximate agreement with his corresponding numerical solutions, both of which are based on an assumption of constant gradient Richardson number at the interface.

The laboratory experiments of *Deardorff and Willis* [1982] did not satisfy the above similarity conditions, since the scaled boundary layer temperature and density gradients varied by an order of magnitude even within the same experiment (Figure 4). The degree of stratification in these laboratory experiments will be measured by $h(\partial\rho/\partial z)/\Delta\rho$, where h is again the depth of the turbulent layer, $\Delta\rho$ is the density jump across the entrainment zone, and $\partial\rho/\partial z$ is the mean density gradient in the half of the boundary layer adjacent to the surface where the density gradient was found to be nearly independent of height. If $\Delta\rho$ is replaced by the total density change across the mixing layer, including the density jump, as shown by *Kundu* [1981], the results remain qualitatively similar to those presented below. There is generally no difficulty in determining $\partial\rho/\partial z$ from actual profiles, since the curvature is normally small sufficiently far from the entrainment interface. When $\partial\rho/\partial z$ is large in the boundary layer interior, $\Delta\rho$ is difficult to estimate. Therefore in ambiguous cases, $\Delta\rho$ is computed from initial profiles by requiring conservation of heat or salinity as did *Deardorff and Willis* [1982] and as schematically illustrated in Figure 3. The boundary layer depth h is taken from Deardorff and Willis.

Since stratification in the boundary layer is maintained by entrainment and associated buoyancy fluxes but limited by turbulent mixing, we will study the scaled density gradient as a function of entrainment velocity divided by turbulent velocity scale. The possible dependence of the scaled density gradient on the entrainment rate scaled by turbulent velocity scale can be more formally argued as follows: During a turbulent time scale δt, δM_α of quantity α is entrained into the thickening boundary layer where

$$\delta M_\alpha \sim w_e \Delta\alpha\, \delta t \qquad (1)$$

w_e is the entrainment rate and $\Delta\alpha$ the jump of property α across the entrainment interface. During time interval δt the entrained amount δM_α is primarily distributed in a region near the entrainment interface of thickness proportional to $v\delta t$, where v is the turbulent velocity scale.

Then the scale value of the entrainment modification of α

TABLE 1. Coefficient of Thermal Expansion for Water

T, °C	α, 10^{-4} °C^{-1}
15	1.60
17	1.90
19	2.12
21	2.32

in the boundary layer near the entrainment interface is

$$\delta\alpha \sim \frac{w_e \Delta\alpha}{v} \tag{2}$$

This modification leads to a bulk gradient of

$$\frac{\overline{\partial\alpha}}{\partial z} = C_\alpha \frac{w_e \Delta\alpha}{vh} \tag{3a}$$

or a scaled gradient of

$$\frac{\overline{\partial\alpha}}{\partial z} h/\Delta\alpha = C_\alpha \, w_e/v \tag{3b}$$

where C_α is a nondimensional parameter.

The above relationship (3*a*) can also be argued from simple dimensional arguments by noting that entrainment acts to create gradients of α while turbulence acts to reduce such gradients through mixing. Relationship (3*a*) could also be argued by assuming that the flux of α into the boundary layer scales with $w_e\Delta\alpha$ (J. Businger and P. Kahn, personal communications). Then (3*a*) would correspond to a flux gradient parameterization with eddy diffusivity proportional to vh.

Relation (3*a*) is similar to that developed by *André et al.* [1979] to describe vertical gradients of moisture mixing ratio in heated atmospheric mixing layers. When made analogous to (3*b*), their relationship is of the form

$$\frac{h}{\Delta q}\frac{\overline{\partial q}}{\partial z} = C_q \, w_e/w_* \tag{4}$$

where q is the specific humidity, w_* is the free convection velocity scale [*Deardorff*, 1970], and C_q has been estimated to be about 10 [*André et al.*, 1979].

In the laboratory experiments analyzed here, turbulence is generated by surface layer shear induced by the surface friction velocity and by shear at the entrainment interface. Choosing the velocity scale to be the surface friction velocity or choosing it to be the shear at the entrainment interface produces analyses which are statistically similar. This is due to the fact that for the data analyzed here, the velocity jump at the entrainment interface is highly correlated with the surface friction velocity although there is some systematic variation in their ratio [*Deardorff and Willis*, 1982, equations (15)–(16)]. Since interfacial shear was not measured in some of the experiments, we proceed by choosing the turbulent velocity scale to be the surface friction velocity. This, of course, does not rule out interfacial shear as an important source of turbulent energy.

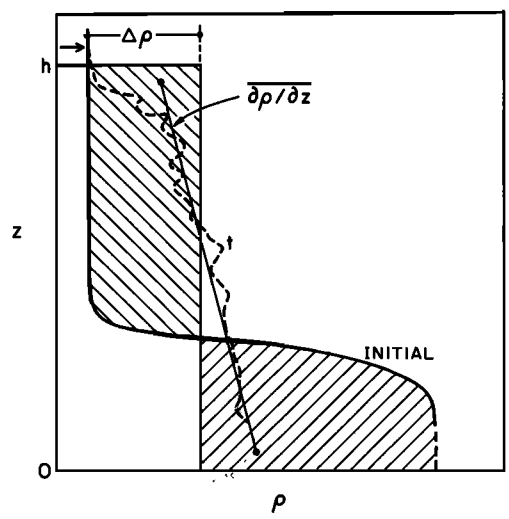

Fig. 3. Determination of scaling parameters from measured density profiles.

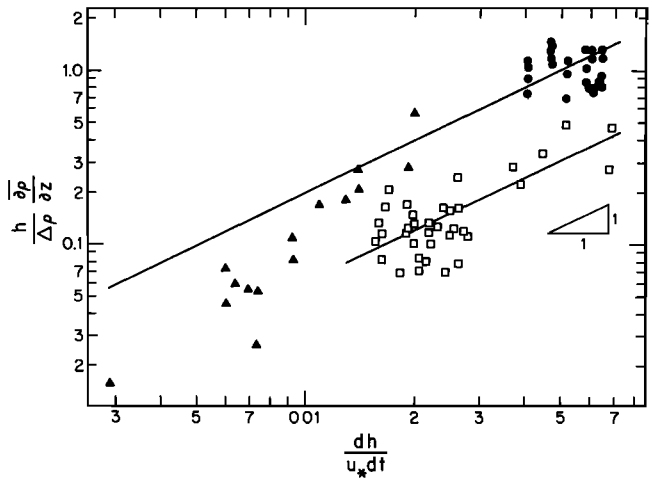

Fig. 4. Scaled density gradient in the interior of the thickening turbulent boundary layer as a function of scaled entrainment rate. Solid symbols correspond to experiments with two layers of different salinity (Kantha: solid circles; Deardorff and Willis, numbers 16 and 17: solid triangles), while open symbols correspond to experiments with an outer thermally-stratified layer (Deardorff and Willis, numbers 1 and 2: open squares). The two solid lines represent the linear relationship (5).

By choosing the turbulent velocity scale to be the surface friction velocity, (3*b*) for density becomes

$$\frac{h}{\Delta\rho}\frac{\overline{\partial\rho}}{\partial z} = C_\rho \frac{w_e}{u_*} \tag{5}$$

For the data analyzed here (Figure 4), the scaled density gradient $(\overline{\partial\rho/\partial z})\,(h/\Delta\rho)$ does indeed increase with increasing values of the entrainment rate scaled by the turbulent velocity scale, although the scatter is significant especially between experiments. Thus with increasing buoyancy flux due to entrainment the turbulence is not able to redistribute the density fast enough to eliminate stratification in the boundary layer.

The somewhat greater scaled density gradient in the temperature-stratified experiments as compared to the two-layer salt-stratified experiments could be related to differences in experimental and analysis procedures. Molecular diffusion is more likely to play an important role in temperature-stratified experiments than in the two-layer salt-stratified experiments. The coefficient of molecular diffusion for heat is two orders of magnitude larger than the one for salt, leading to values of the Peclet number $Pe = w_e\, h/\nu_\alpha$ of the order of 200 for temperature-stratified experiments and of order 20,000 for salt-stratified experiments. The influence of molecular diffusion on the entrainment dynamics has been conjectured by *Turner* [1968] and documented by *Crapper and Linden* [1974] and *Wolanski and Brush* [1975], who showed that the dimensionless entrainment velocity varies, for a given overall Richardson number, by two orders of magnitude when the coefficient of molecular diffusion is

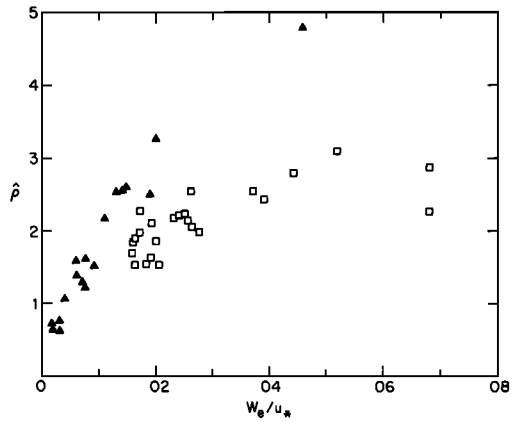

Fig. 5. Integral stratification parameter $\hat{\rho}$ as a function of scaled entrainment rate for salt stratification (solid triangles) and thermal stratification (open squares).

changed from 10^{-3} (for heat) to 10^{-9} (for natural kaolinite clay).

The difference between the two-layer salt-stratified values computed from *Kantha* [1978] and those computed from *Deardorff and Willis* [1982] may be due to stronger curvature effects in the Kantha experiments. *Price* [1979] and *Thompson* [1979] have shown that sidewall friction significantly influences entrainment dynamics. An additional complication is that inertial stability in annulus experiments may lead to a preferred region for entrainment adjacent to the outer wall (J. W. Deardorff, private communication). Then boundary layer stratification could be a function of distance in the radial direction. The differences between the two kinds of experiments could also be due to differences in the overall dynamical behavior between two-layer and linearly stratified systems. *Kundu*'s [1981] analysis indicates that two-layer systems are characterized by density gradients which decrease with time and which consequently may become significantly smaller than those corresponding to linearly stratified experiments.

Figure 4 suggests a roughly linear relationship between scaled density gradient and scaled entrainment rate, so that $C\rho$ in (5) can be evaluated. This parameter is about 20 for two-layer salt-stratified flows and approximately 6 for linear temperature-stratified flows. In the case of the salt-stratified experiments the simple linear law with $C_\rho = 20$ has been fitted with particular concern to the rapidly growing turbulent boundary layers. It seems to overestimate the very small density gradients found in slowly evolving turbulent boundary layers. These values are comparable to those of *André et al.* [1979], except that with the laboratory data, C_ρ is found to decrease when the overall Richardson number increases. This dependence explains part of the scatter in Figure 4. It may be that entrainment compared to mixing within the boundary layer is generated less effectively with large Richardson number. If a sufficient data sample becomes available, it would be useful to examine the simultaneous dependence of the scaled density gradient on all the nondimensional numbers which are thought to be relevant.

4. Integral Properties

While the density gradient is nearly constant and easy to compute in the boundary layer sufficiently far from the entrainment interface, this gradient increases as the interface is approached. In fact, it is often difficult to separate the density jump from this region of increasing density gradient. This problem can be avoided by defining certain bulk or integral parameters describing stratification. As an example, we evaluate the scaled layer averaged value of the deviation of density from its surface value ρ_{sfc}

$$\hat{\rho} \equiv [h(\rho(h) - \rho_{sfc})]^{-1} \int_0^h (\rho(z) - \rho_{sfc})\, dz \qquad (6)$$

For thermally stratified experiments, $\hat{\rho}$ can be computed from the temperature distribution by using the Boussinesq approximation, in which case,

$$\hat{\rho} = [h(T(h) - T_{sfc})]^{-1} \int_0^h (T(z) - T_{sfc})\, dz$$

The stratification parameter $\hat{\rho}$ vanishes in the case of well-mixed boundary layer flow and is otherwise expected to be positive and bounded by unity. For these calculations, h is chosen to be the free flow (unmodified) side of the inversion layer so as to include all of the turbulent stratified flow (see the horizontal arrow in Figure 3). Such a determination of this edge of the entrainment region was normally quite obvious in the unsmoothed profiles from *Deardorff and Willis* [1982].

For the salt-stratified experiments, computed values of the stratification parameter $\hat{\rho}$ increase with increasing scaled entrainment rate with a slightly less than linear dependence (Figure 5). For the thermally stratified experiments, $\hat{\rho}$ increases less rapidly with (w_e/u_*). In fact, $\hat{\rho}$ reaches a maximum value of about 0.3 after the entrainment rate exceeds a value of 4 or 5% of the friction velocity.

Figure 5 also suggests that the boundary layer becomes well mixed ($\hat{\rho} \to 0$) as w_e/u_* approaches zero. Slow entrainment rate and strong turbulence are most likely to simultaneously occur with strong density jump at the interface. The

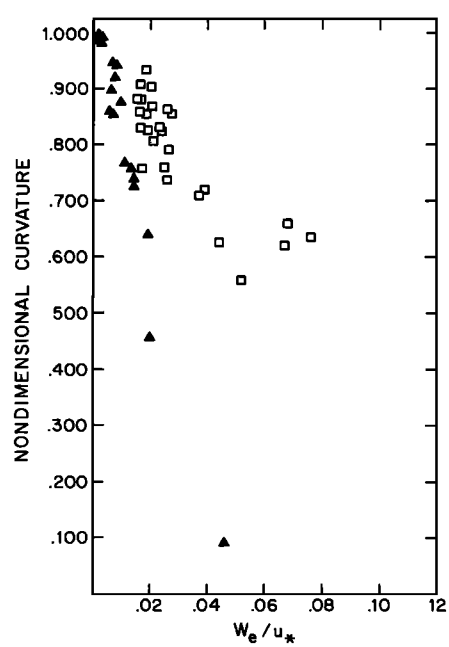

Fig. 6. Scaled curvature $\tilde{\rho}$ as a function of scaled entrainment rate for salt stratification (solid triangles) and thermal stratification (open squares).

measured value of $\hat{\rho}$ would never precisely approach zero, since the measured entrainment interface will always have finite thickness due to instrumental smoothing and molecular diffusion.

The above stratification parameter $\hat{\rho}$ describes the bulk stratification but does not contain any information about vertical structure. For weak entrainment rates relative to the strength of the turbulence the nonzero value of the stratification parameter is due mainly to the nonzero thickness of the density transition, while gradients remain small in most of the boundary layer. With increased relative entrainment rate, the significant stratification extends throughout the boundary layer.

The behavior of this vertical structure can be studied by computing the nondimensional curvature

$$\tilde{\rho} = \frac{\rho(h) - 2\rho(h/2) + \rho_{sfc}}{\rho(h) - \rho_{sfc}} \simeq \frac{T(h) - 2T(h/2) + T_{sfc}}{T(h) - T_{sfc}} \quad (7)$$

The nondimensional curvature $\tilde{\rho}$ vanishes in the case of constant stratification throughout the boundary layer. This parameter increases as the stratification becomes concentrated near the entrainment interface approaching unity in the well-mixed case.

The observed curvature (Figure 6) decreases rapidly as the scaled entrainment rate increases, reflecting extension of stratification from the entrainment region into the boundary layer. Sufficiently strong entrainment rate in the salt-stratified experiments leads to very small curvature corresponding to almost constant stratification throughout the boundary layer. As with other stratification parameters, the boundary layer structure in the thermally stratified experiments show less response to increasing entrainment rate.

5. Concluding Remarks

These results indicate that as the entrainment rate increases relative to the strength of the turbulence, the turbulence can no longer maintain a well-mixed state in temperature or density. In other terms, the entrainment leads to a buoyancy flux at the interface and subsequent stratification of the boundary layer. With weak entrainment rates this boundary layer stratification can be viewed as extension or thickening of the density transition. If the entrainment rate becomes sufficiently rapid, this thickening influences the entire boundary layer. The extension of stratification into the boundary layer probably leads to weaker turbulence in the boundary layer, at least for a given value of u_*. This reduces the transport of turbulence energy toward the entrainment interface, which acts to restrict the further increase of w_e/u_* with decreasing interfacial Richardson number. The effect of this boundary layer stratification may have been included in previous mixed layer growth models, perhaps unknowingly, by using experimental data to adjust the available coefficients or the power of dependence on the interfacial Richardson. It may be useful to parameterize such boundary layer stratification more directly.

Acknowledgments. The authors would like to thank J. Deardorff and G. Willis for helpful comments and for providing us with their original experimental data. This material is based upon work supported by the National Science Foundation under Grants ATM 7908308 and ATM 8109778 and Direction de la Météorologie, Paris. J. C. André performed this work while on leave from the latter organization.

References

André, J. C., P. Lacarrère, and L. J. Mahrt, Sur la distribution verticale de l'humidité dans une couche limite convective, *J. Rech. Atmos., 13,* 135–146, 1979.

Artaz, M. A., and J. C. André, Similarity studies of entrainment in convective mixed layers, *Boundary Layer Meteorol., 19,* 51–66, 1980.

Crapper, P. F., and P. F. Linden, The structure of turbulent density interfaces, *J. Fluid Mech., 65,* 45–63, 1974.

Deardorff, J. W., Convective velocity and temperature scales for the unstable planetary boundary layer and for Rayleigh convection, *J. Atmos. Sci., 27,* 1211–1213, 1970.

Deardorff, J. W., and G. E. Willis, Dependence of mixed-layer entrainment on shear stress and velocity jump, *J. Fluid Mech., 115,* 123–149, 1982.

Hopfinger, E. J., and P. F. Linden, Formation of thermoclines in zero-mean-shear turbulence subjected to a stabilizing buoyancy flux, *J. Fluid Mech., 114,* 157–173, 1981.

Kantha, L. H., On surface-stress-induced entrainment at a buoyancy interface, *Rep. GFDL TR 78-1,* Dep. Earth Planet. Sci., Johns Hopkins Univ., 1978.

Kundu, P. K., Self-similarity in stress-driven entrainment experiments. *J. Geophys. Res., 86,* 1979–1988, 1981.

Niiler, P. P., and E. B. Kraus, One-dimensional model of the upper ocean, in *Modelling and Prediction of the Upper Layers of the Ocean,* pp. 143–172, Pergamon, Oxford, 1977.

Price, J. F., On the scaling of stress-driven entrainment experiments, *J. Fluid Mech., 90,* 509–529, 1979.

Stull, R. B., Mixed-layer depth model based on turbulent energetics, *J. Atmos. Sci., 33,* 1268–1278, 1976.

Tennekes, H., and A. G. M. Driedonks, Basic entrainment equations for the atmospheric boundary layers, *Boundary Layer Meteorol., 20,* 515–531, 1981.

Thompson, R. O. R. Y., A re-interpretation of the entrainment process in some laboratory experiments, *Dyn. Atmos. Oceans, 4,* 45–55, 1979.

Turner, J. S., The influence of molecular diffusivity on turbulent entrainment across a density interface, *J. Fluid Mech., 33,* 639–656, 1968.

Wolanski, E. J., and L. M. Brush, Jr., Turbulent entrainment across stable density step structures, *Tellus, 27,* 259–268, 1975.

(Received March 4, 1982;
revised November 8, 1982;
accepted November 9, 1982.)